NATIONAL ADVISORY COMMITTEE FOR AERONAUTICS

TECHNICAL MEMORANDUM

No. 1159

WIND-TUNNEL MEASUREMENTS ON THE HENSCHEL MISSILE "ZITTERROCHEN" IN SUBSONIC AND SUPERSONIC VELOCITIES

By Weber and Kehl

Translation
"Windkanalmessungen am Henschel-Gerät 'Zitterrochen' bei Unter- und Überschallgeschwindigkeiten"

and

WIND-TUNNEL MEASUREMENTS ON THE WING OF THE HENSCHEL MISSILE "ZITTERROCHEN" IN SUBSONIC AND SUPERSONIC VELOCITIES

By Kehl

Translation
"Windkanalmessungen am Flügel des Henschelgerätes 'Zitterrochen' bei Unter- und Überschallgeschwindigkeiten"

Washington

April 1948

NATIONAL ADVISORY COMMITTEE FOR AERONAUTICS

TECHNICAL MEMORANDUM NO. 1159

WIND-TUNNEL MEASUREMENTS ON THE HENSCHEL MISSILE

"ZITTERROCHEN"[1] IN SUBSONIC AND

SUPERSONIC VELOCITIES*

By Weber and Kehl

Abstract: At the request of the Henschel Aircraft Works,
A. G. Berlin, three models of the missile
"Zitterrochen" were investigated at subsonic
velocities (open jet 215-millimeter diameter)
and at supersonic velocities (open jet 110
by 130 millimeters) in order to determine the
effect of various wing forms on the air forces
and moments. Three-component measurements
were taken, and one model was also investi-
gated with deflected control plates.

Outline: I. Relations and Definitions

II. Description of Model and Measured Results

I. RELATIONS AND DEFINITIONS

A   lift, component of the air forces perpendicular
to the direction of flow, kilograms

W   drag, component of the air forces in the
direction of flow, kilograms

---

[1]Literally "trembling ray." (This type of ray is
that which lives in the ocean. Presumably the name
originated because of the triangular shape of the ray.)

M_0 moment, referred to the projectile body,
        kilogram-meters

f distance of the pressure point from the rear
        edge of the projectile, meters

D caliber of the projectile body, meters

F cross-sectional area of the projectile,
        meters^2 $\dfrac{D^2}{4\pi}$

ρ density of air (kg sec^2 m^{-4})

v stream velocity (m sec^{-1})

a velocity of sound (m sec-^{1})

α angle of attack, degrees

M Mach number (v/a)

c_a lift coefficient $\left(\dfrac{A}{\dfrac{\rho}{2}v^2 F}\right)$

c_W drag coefficient $\left(\dfrac{W}{\dfrac{\rho}{2}v^2 F}\right)$

c_{m_0} moment coefficient $\left(\dfrac{M_0}{\dfrac{\rho}{2}v^2 FD}\right)$

II. DESCRIPTION OF MODEL AND MEASURED RESULTS

The models tested are illustrated in figures 1 to 3.
They differ only in wing form; the projectile bodies are
all the same. The wings have about the same area, but
the aspect ratios are different (2.0, 1.0, 0.5) and the
thickness ratios are different. The profiles of the
wing are the same all along the span. For the measurements
at $M < 1$ a model length of 200 millimeters and for
$M > 1$ a model length of 80 millimeters was chosen

(corresponding to projectile diameters of 20.4 and 8.2 millimeters, respectively). The Reynolds numbers based on the length of the body of the projectile are

R	M
2×10^6	0.5×10^6
3.1	.9
1.3	1.5
1.1	2.0

The models were supported at the stern by an inclined strut. At subsonic velocities (open jet 215-millimeter diameter) measurements were conducted at $M = 0.5$, 0.8, 0.85, and 0.9. Tunnel corrections were not used. At supersonic velocities measurements were taken at $M = 1.45$ and 1.99. The angle of attack was varied from $0°$ to $10°$.

In figures 4 to 10 the lift coefficient c_a, drag coefficient c_w, moment coefficient c_{m_o}, and the position of the pressure point $\frac{f}{D} = \frac{c_{m_o}}{c_n}$ ($c_n = c_a \cos \alpha + c_w \sin \alpha$) are given for the three different models at constant Mach numbers, so that the effect of various wing forms is visible. With increasing aspect ratio the values $dc_a/d\alpha$ and $dc_{m_o}/d\alpha$ increased for all Mach numbers investigated; furthermore, the drag coefficient also increased, particularly at large angles of attack in the subsonic region and on the other hand, even at $\alpha = 0$ for the supersonic region on account of the larger thickness ratios.

The pressure point shifted forward at all velocities as the aspect ratio was increased.

In figures 11 to 13 the same measured results are presented against Mach number. In the subsonic region the lift coefficients show an increasing trend with increasing Mach number in the sense of Prandtl's equation. No significant decrease in the lift coefficient was observed when approaching the velocity of sound over the range of velocities investigated; however, it is to be noted that on account of not observing the jet corrections the results at $M = 0.9$ are uncertain. Over the range

of supersonic velocities investigated the lift coefficients
for the same angle of attack are of the same magnitude
as in the subsonic region.

The drag coefficient at small angles of attack
slightly decreases with increasing Mach number, which is
explained by the Reynolds number effect on the flow about
the wing. At $M > 1$ the drag coefficients are naturally
higher, since even in a frictionless fluid a drag would
result on account of the finite thickness.

The pressure point of forms ZR 2.0 and ZR 1.0
are independent of the angle of attack and in the subsonic
region it lies about 0.2 D closer to the projectile
point than at supersonic velocities. For the form
ZR 0.5 a shift of the pressure point forward was
observed as the angle of attack was decreased.

In order to obtain a general idea of the effectiveness
of control plates, the model ZR 2.0 was tested with
deflected control plates at $M = 0.7, 0.85, 1.45$, and 1.99.
The measurements of the deflected control plates are
given in figure 1. In figures 14 to 17 the measured
results are presented against angle of attack. As was
to be expected, the effectiveness of the control plates
was less in the supersonic regions than at velocities
below that of sound.

In figures 4 to 17, again it is pointed out that
the curves of the force and moment coefficients use as a
reference area the projectile cross section $(\pi/4)D^2$
and as a reference length the caliber D, as is generally
done for projectiles.

Translated by Chance-Vought
Aircraft Corporation
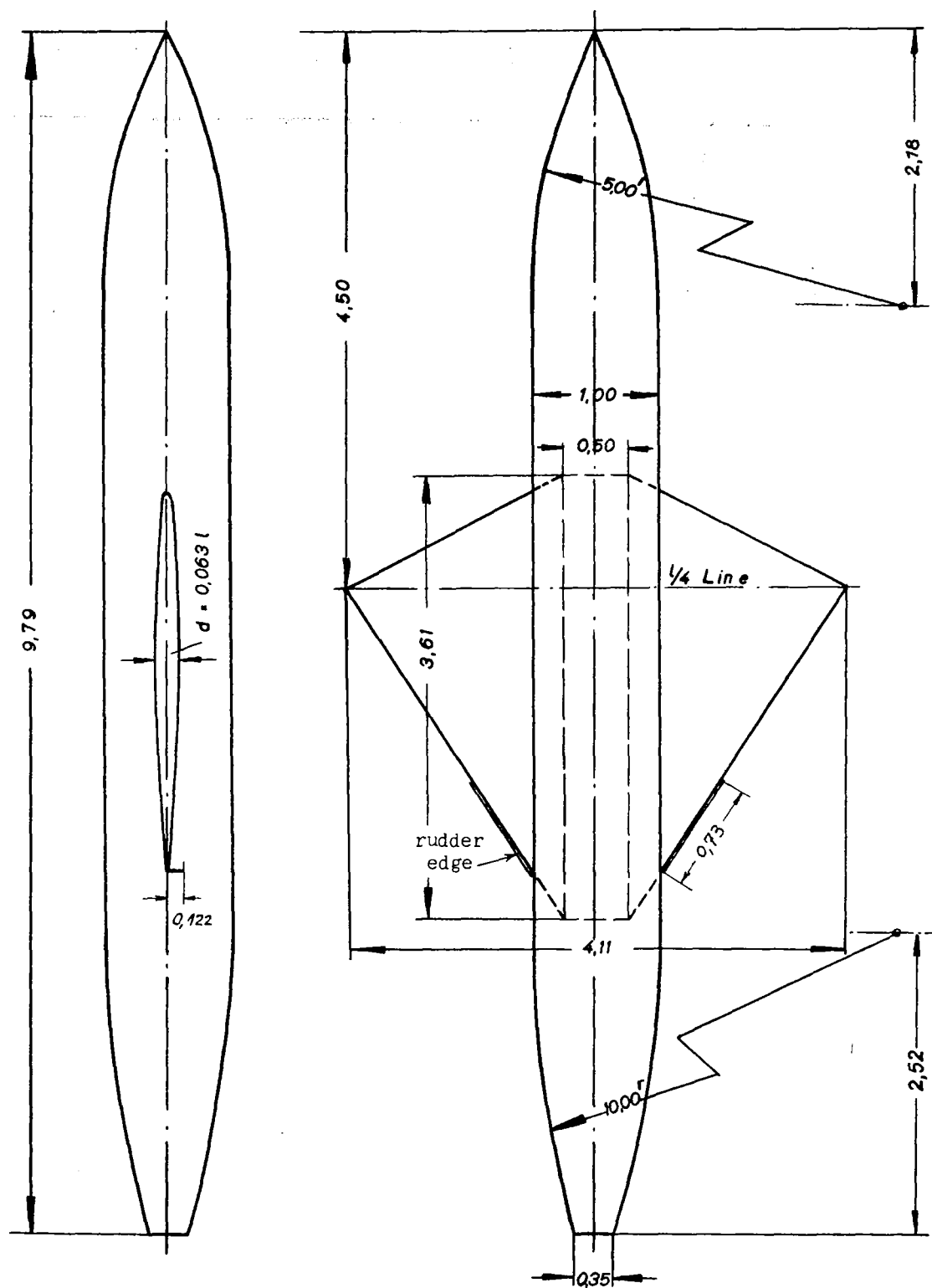
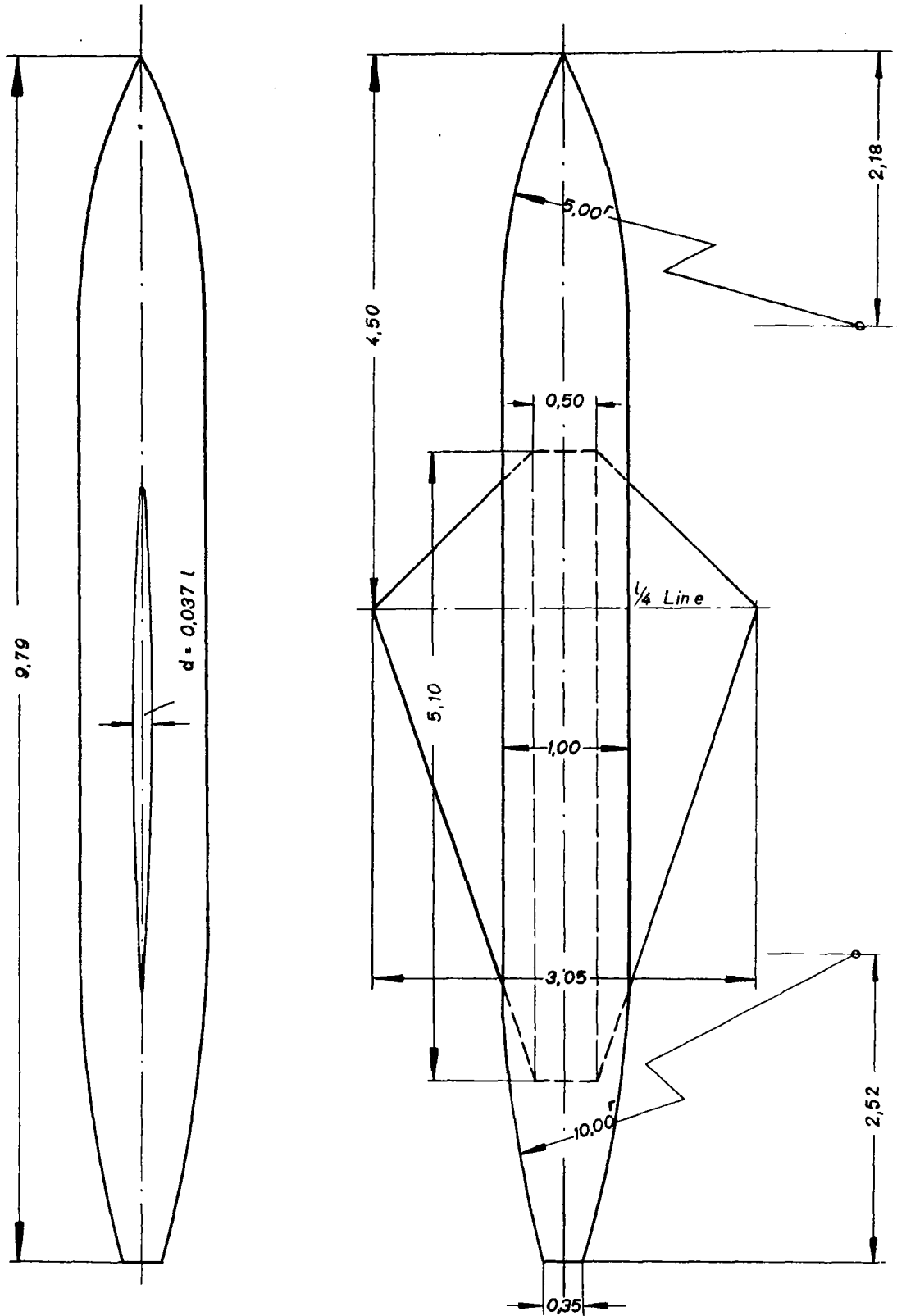Figure 1.- Model ZR-2.0 according to drawing No. FA-SK 280.

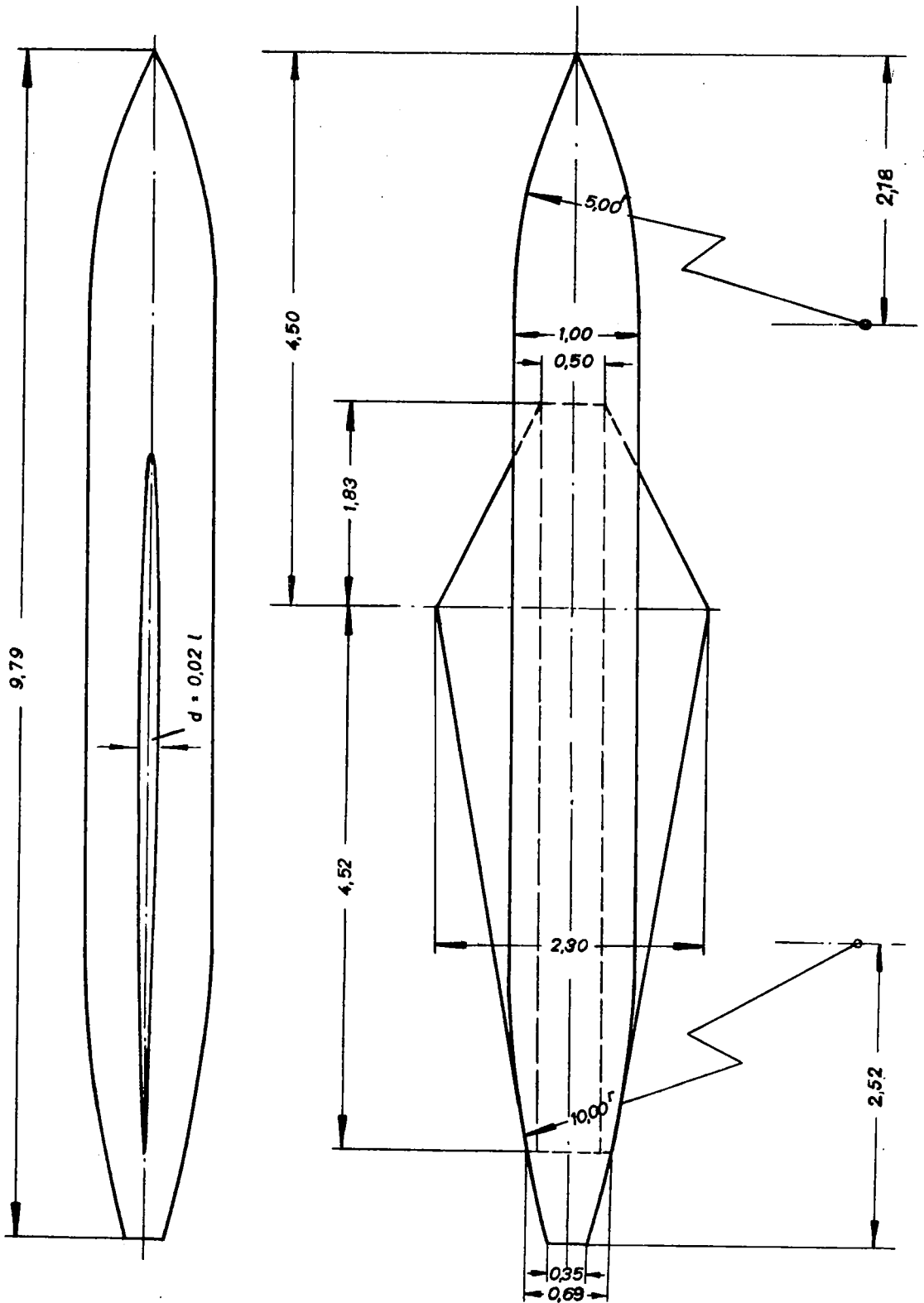Figure 2.- Model ZR-1.0 according to drawing No. FA-SK 279.

Figure 3.-　Model ZR-0.5 according to drawing No. FA-SK 278.

$M = 0.5$
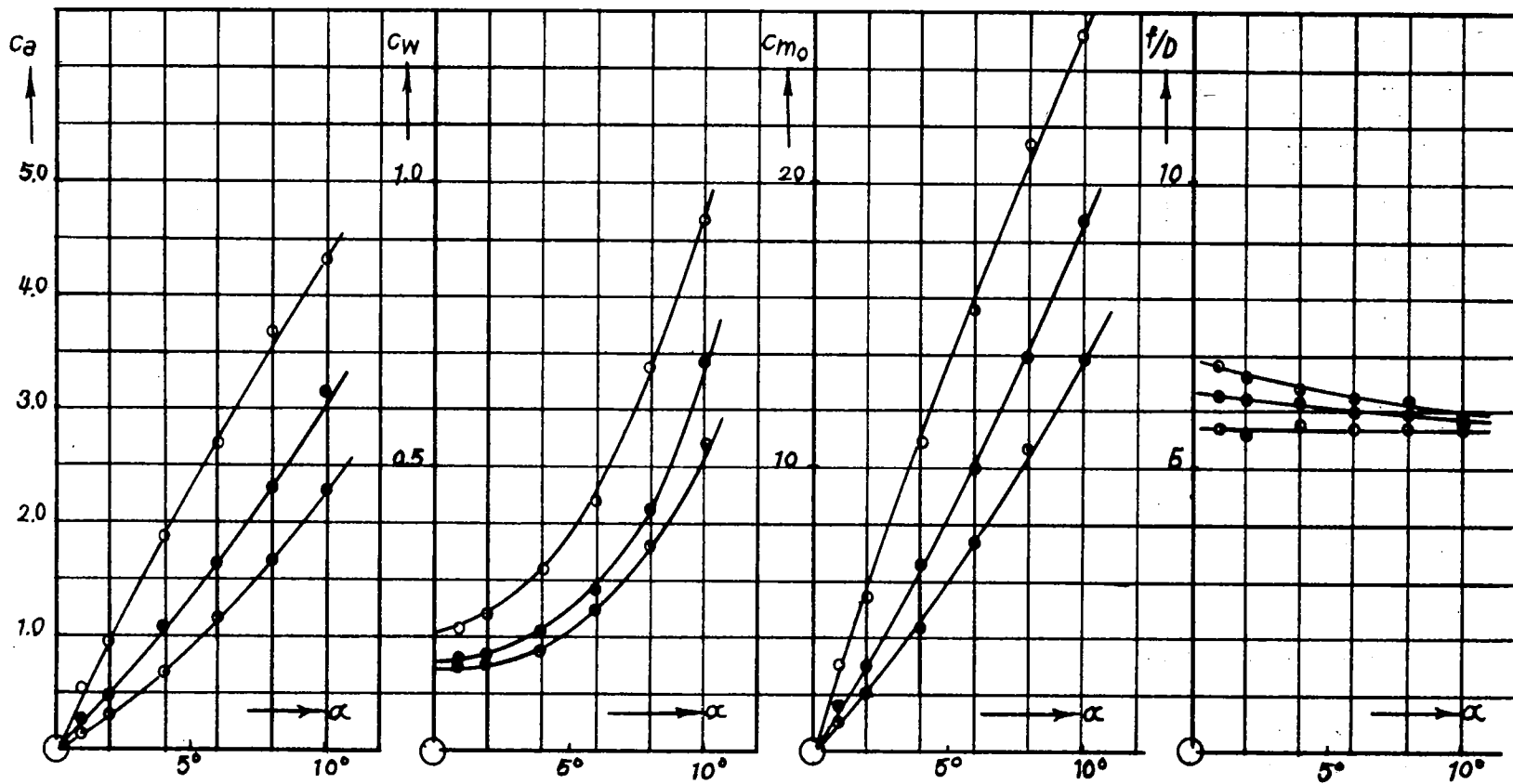
Figure 4.

$M = 0.7$

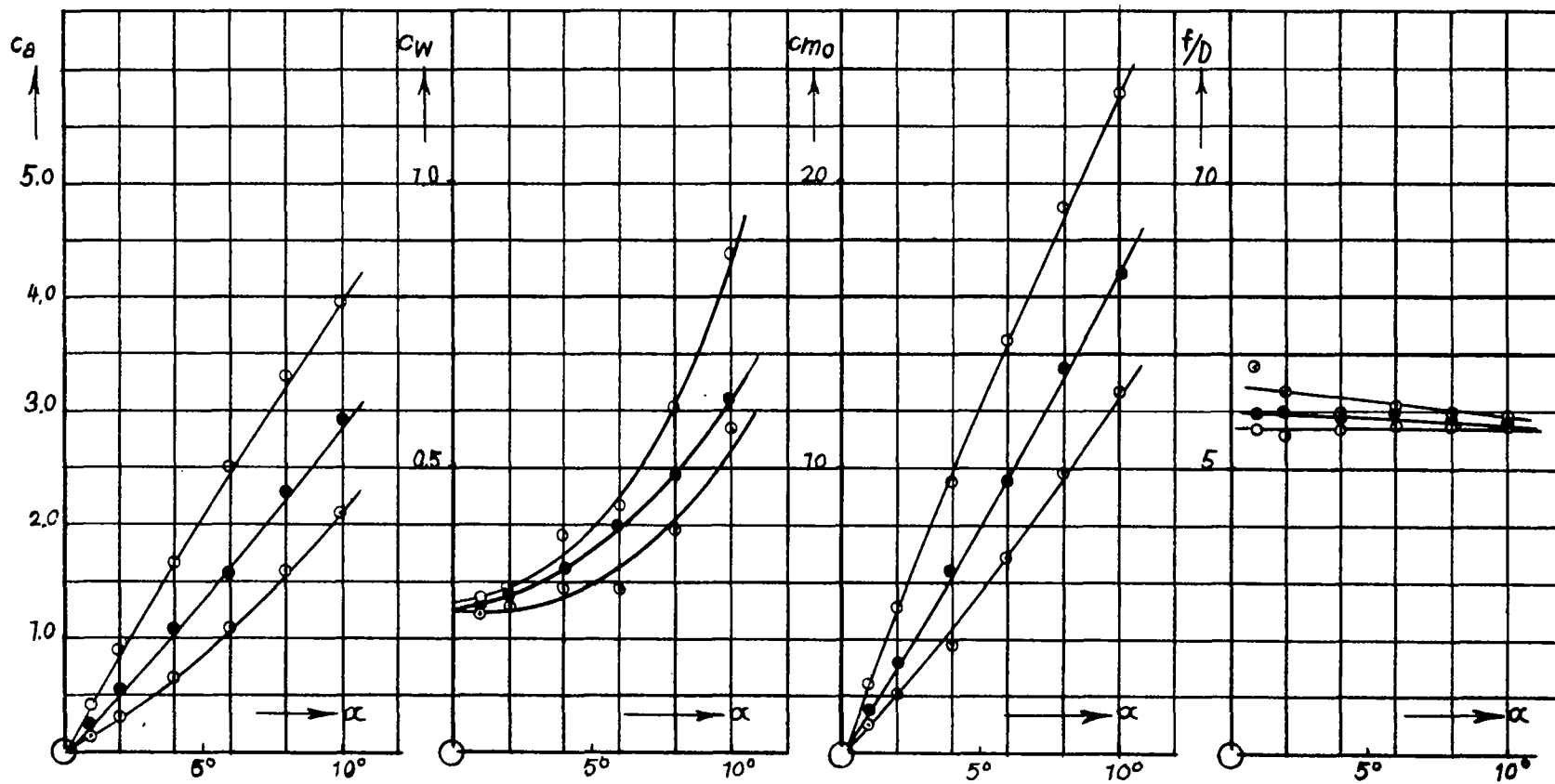Figure 5.

$$M = 0.8$$

Figure 6.

M = 0.85

Figure 7.

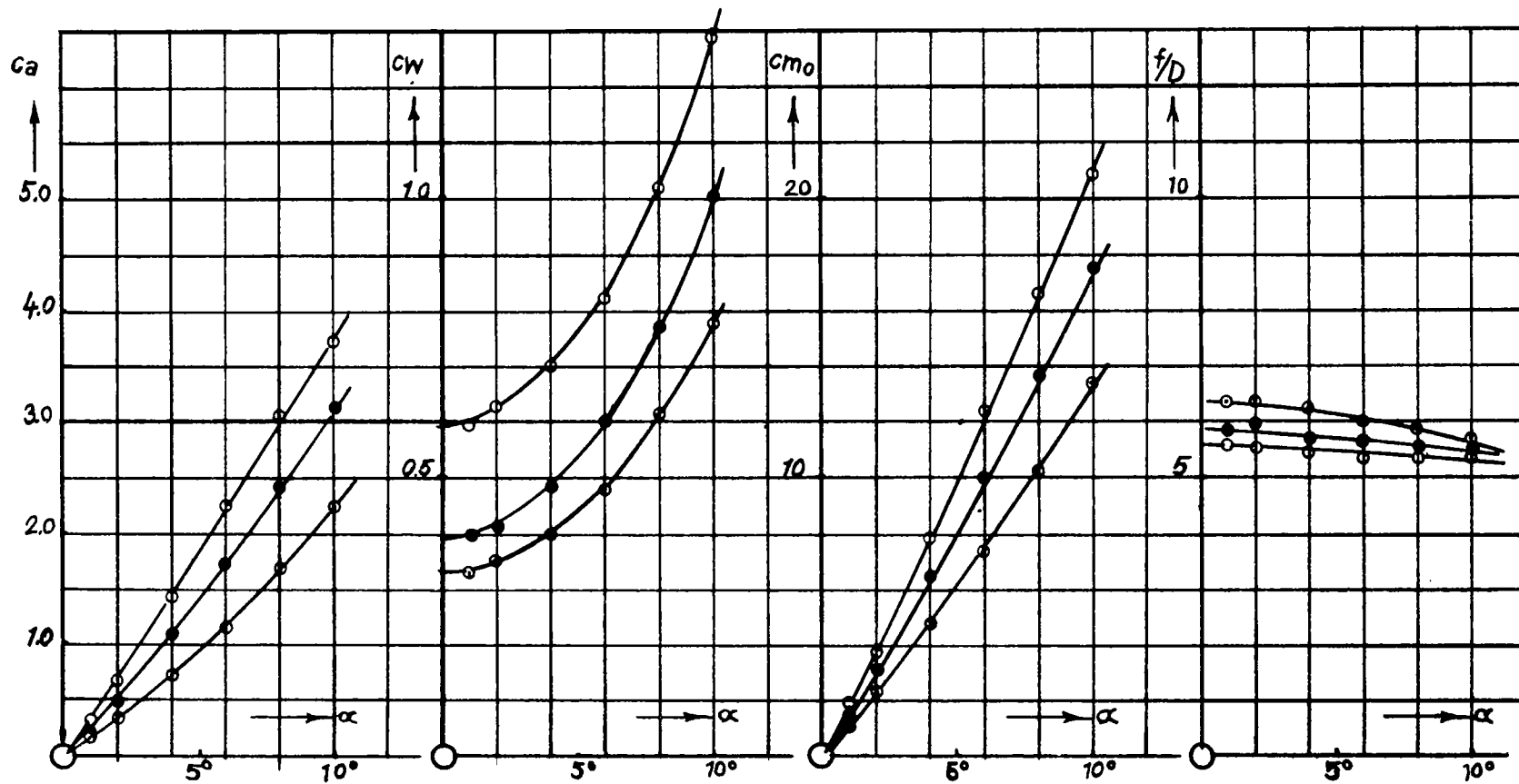$$\underline{M = 0.9}$$
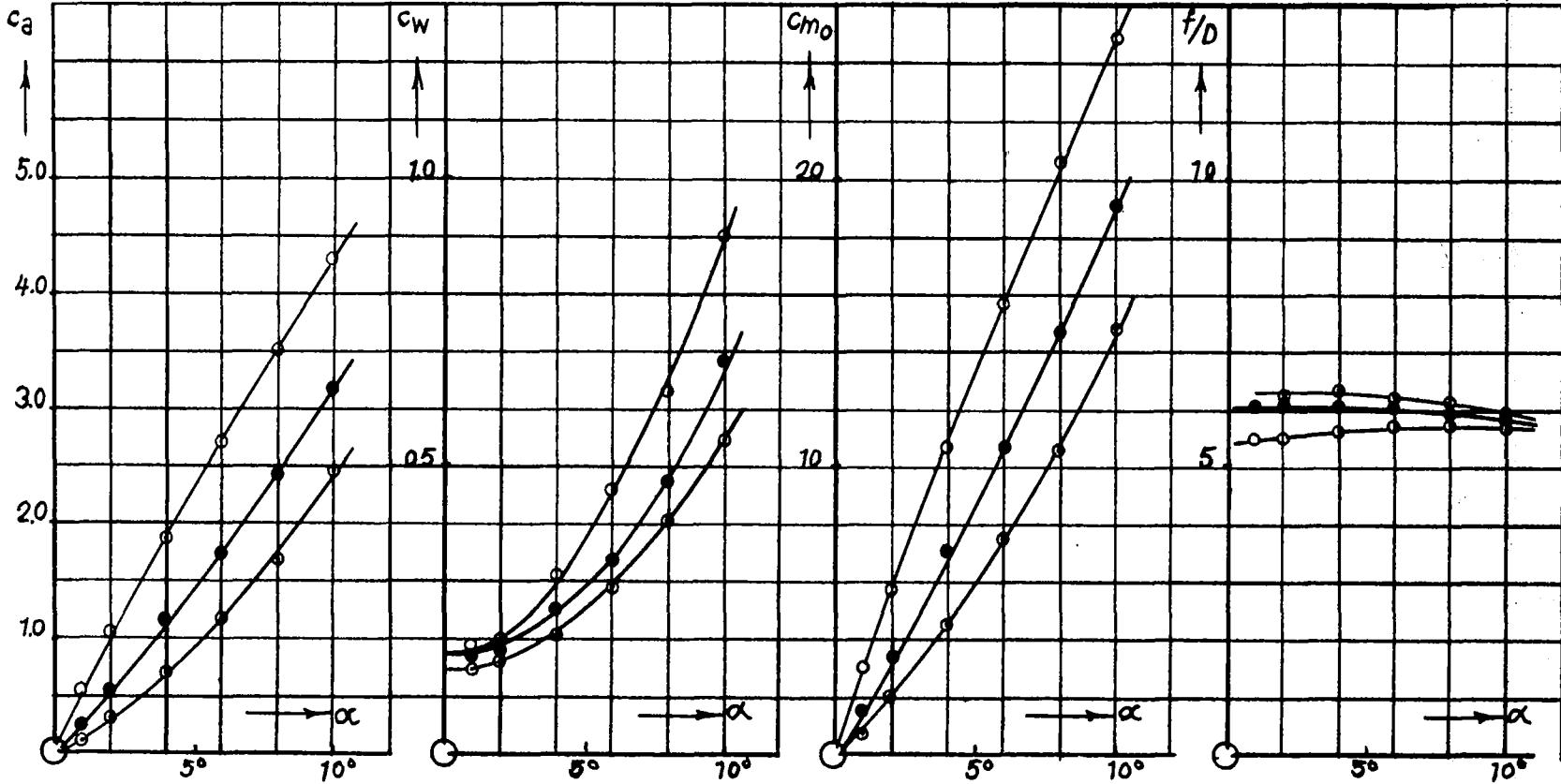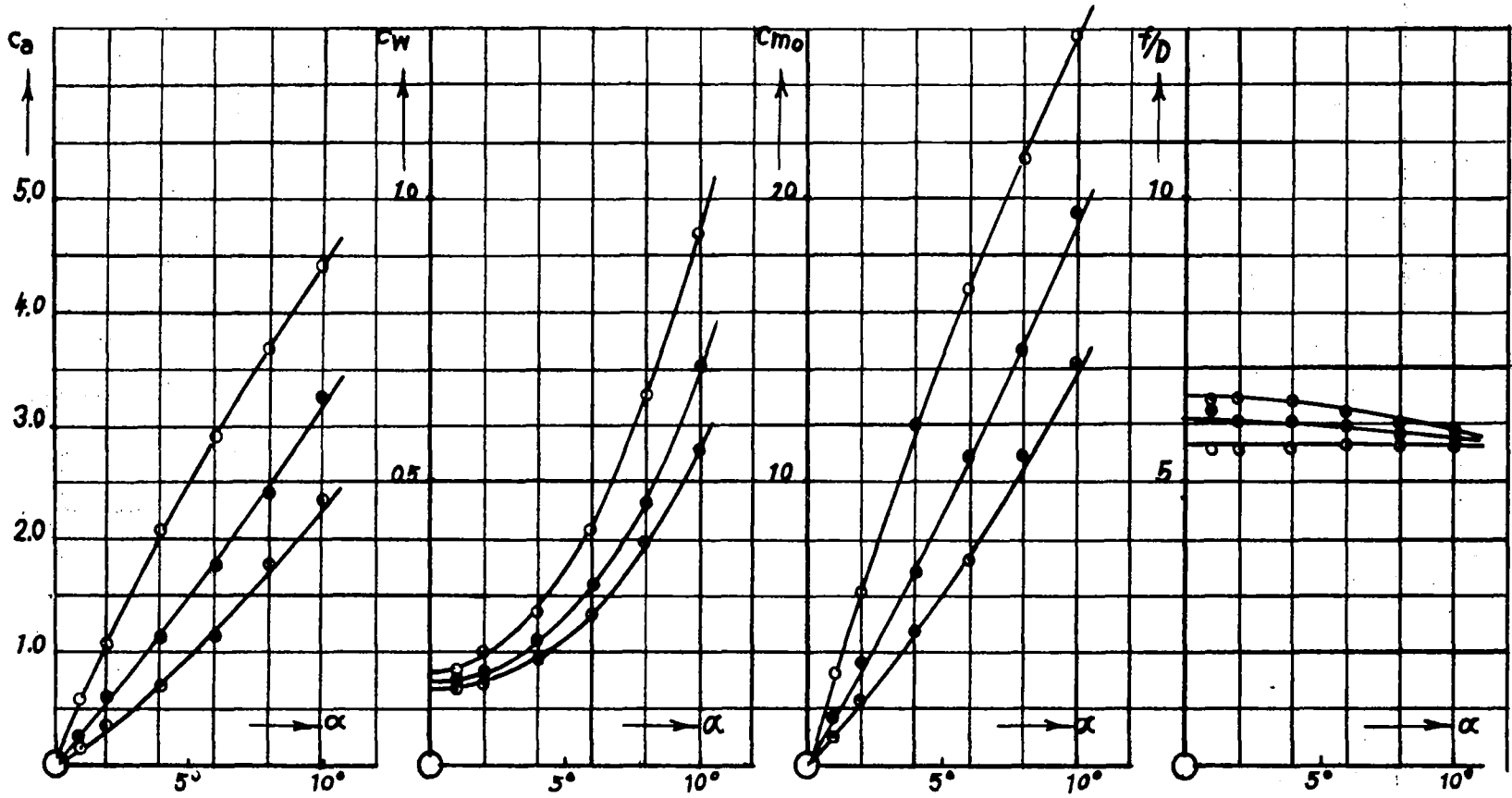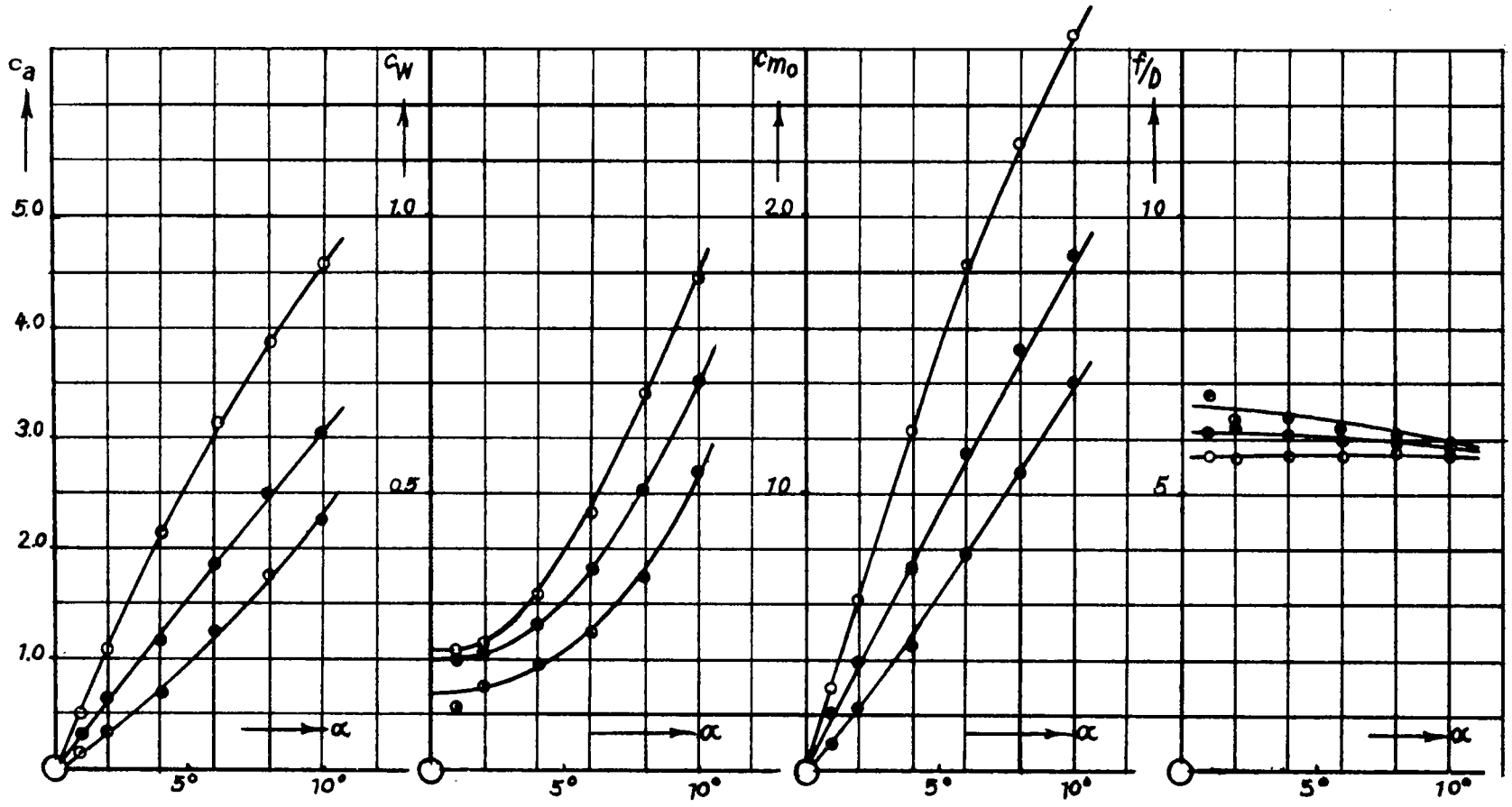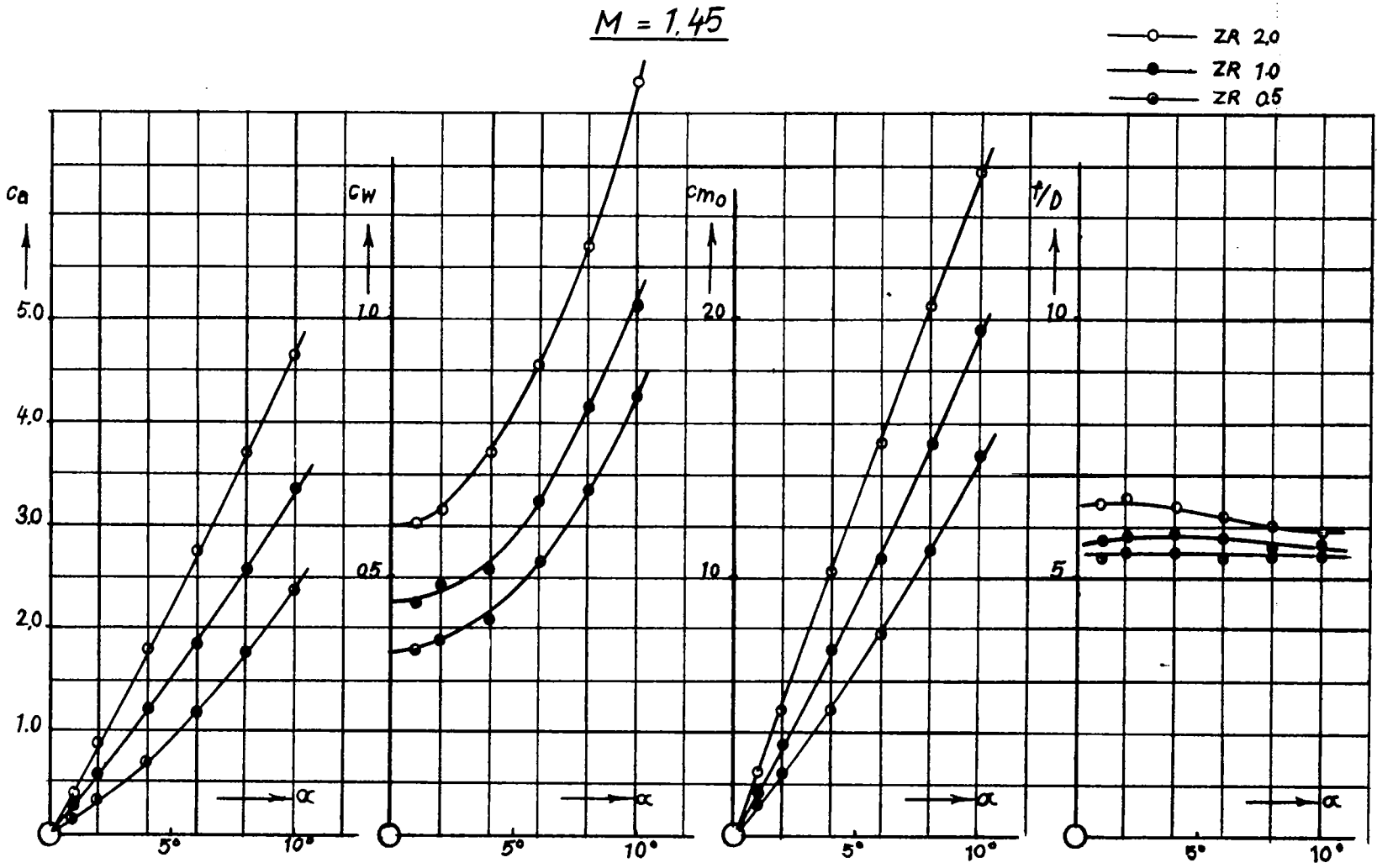
Figure 8.

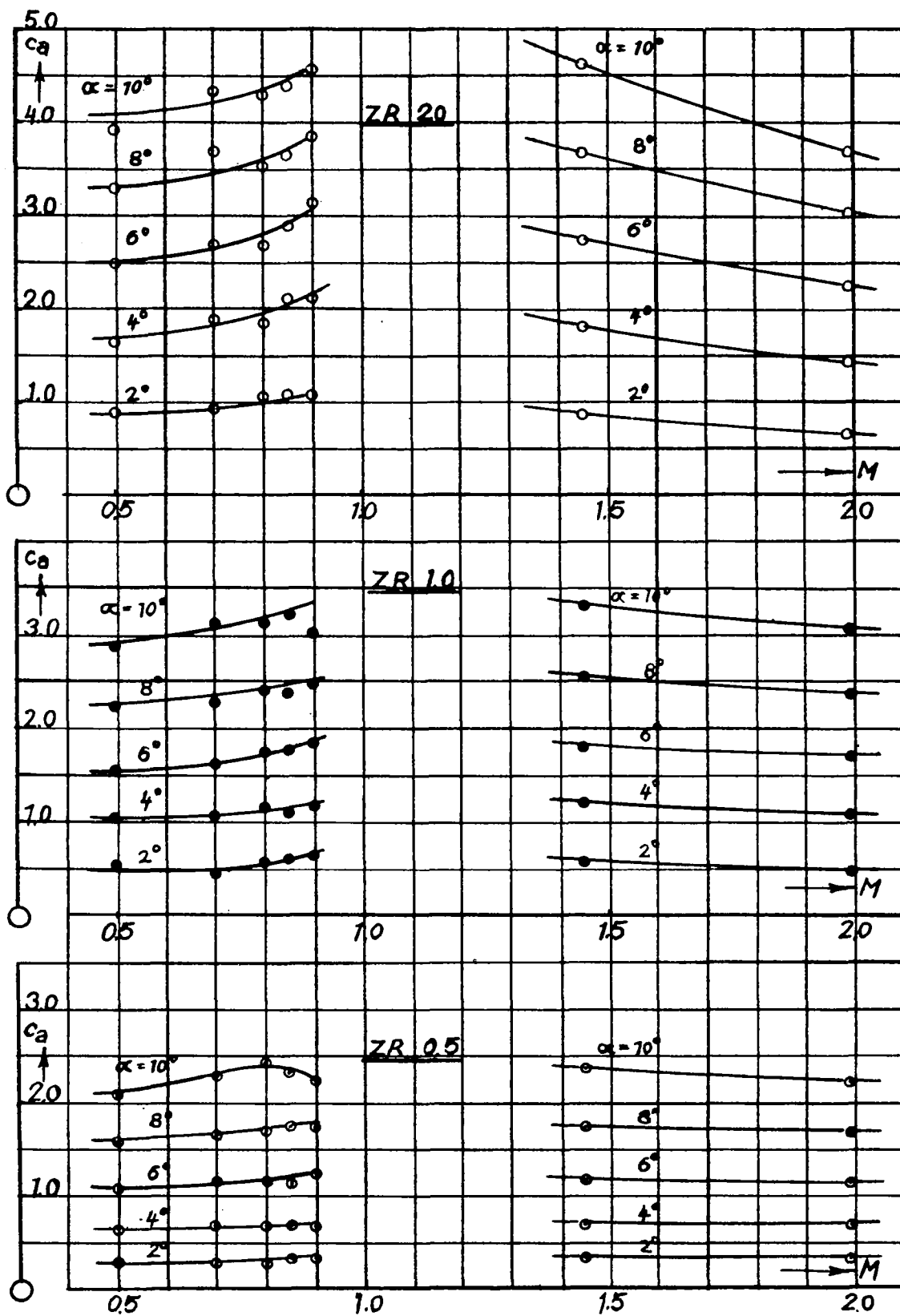Figure 9.

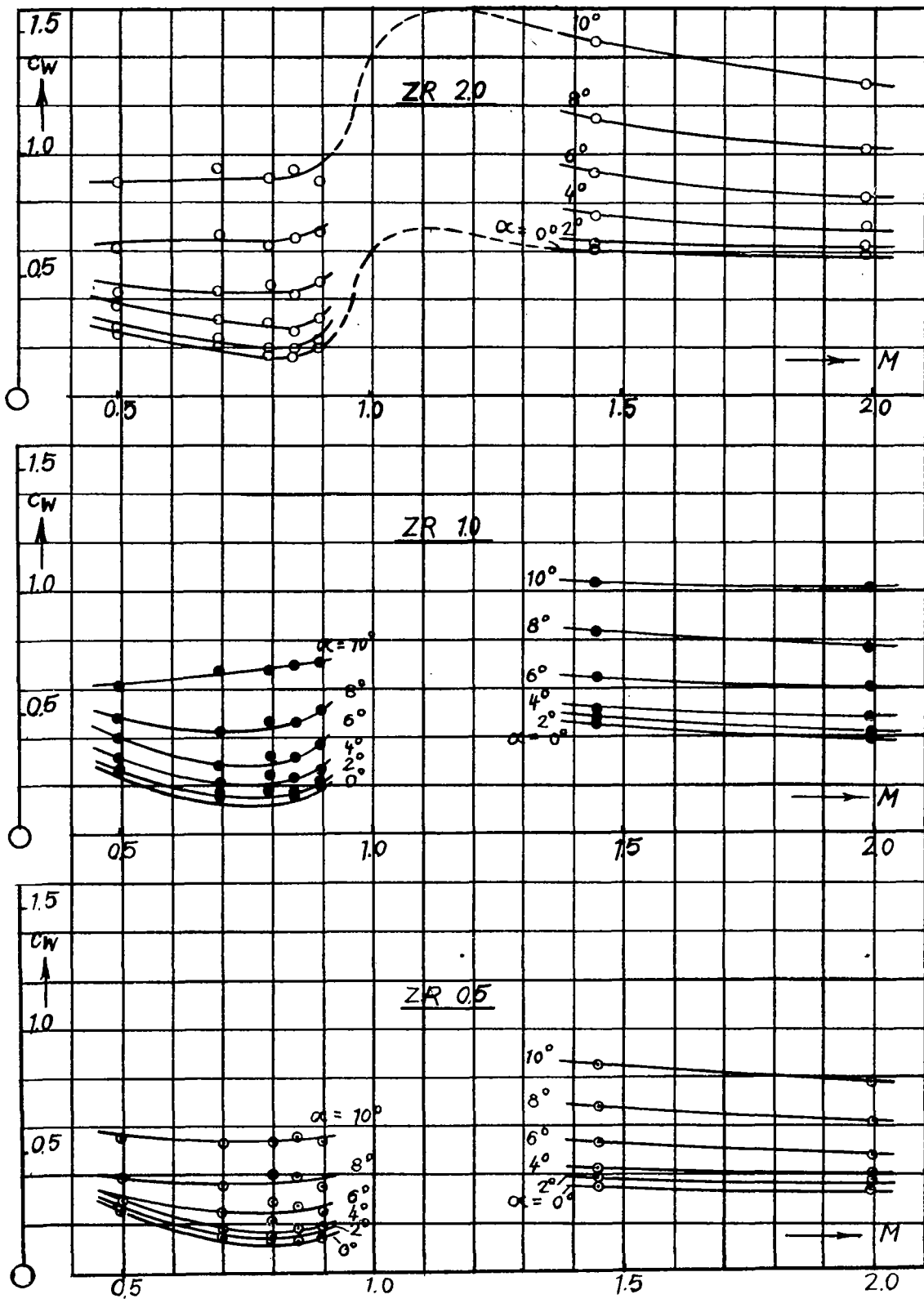## M = 1.99

Figure 10.

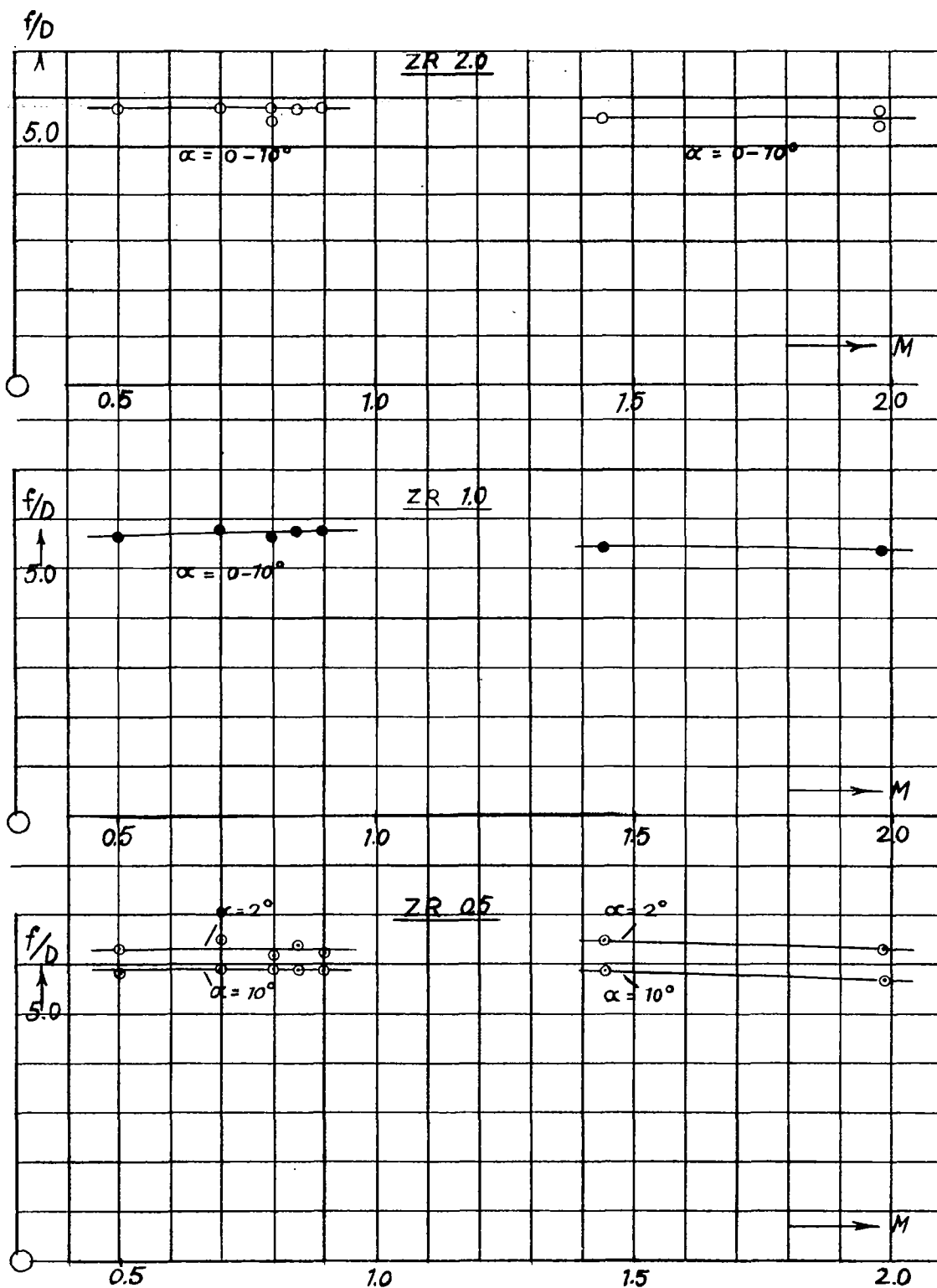Figure 11.-   Lift coefficients.

Figure 12.- Drag coefficients.
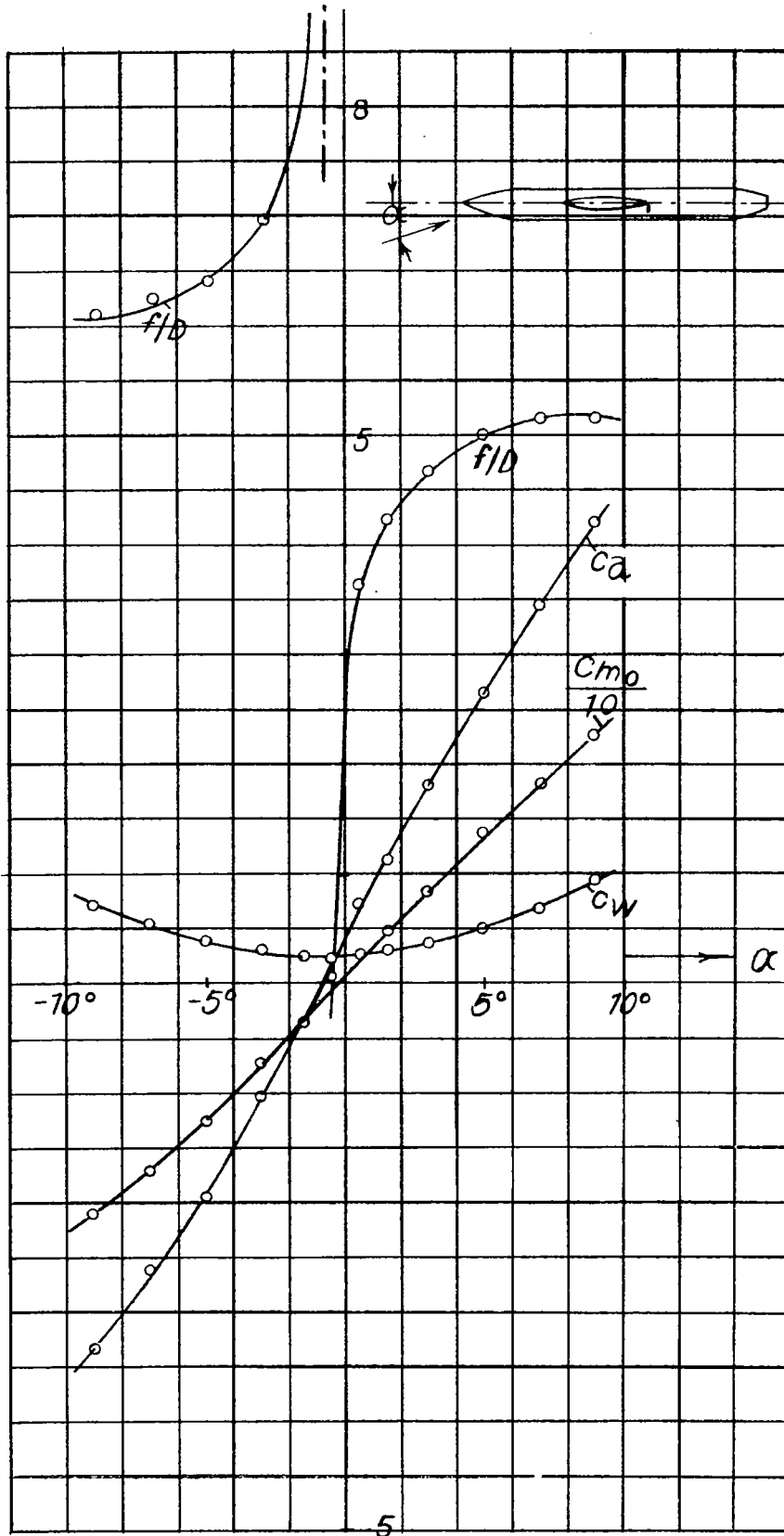
Figure 13.-   Positions of the center of pressure point.

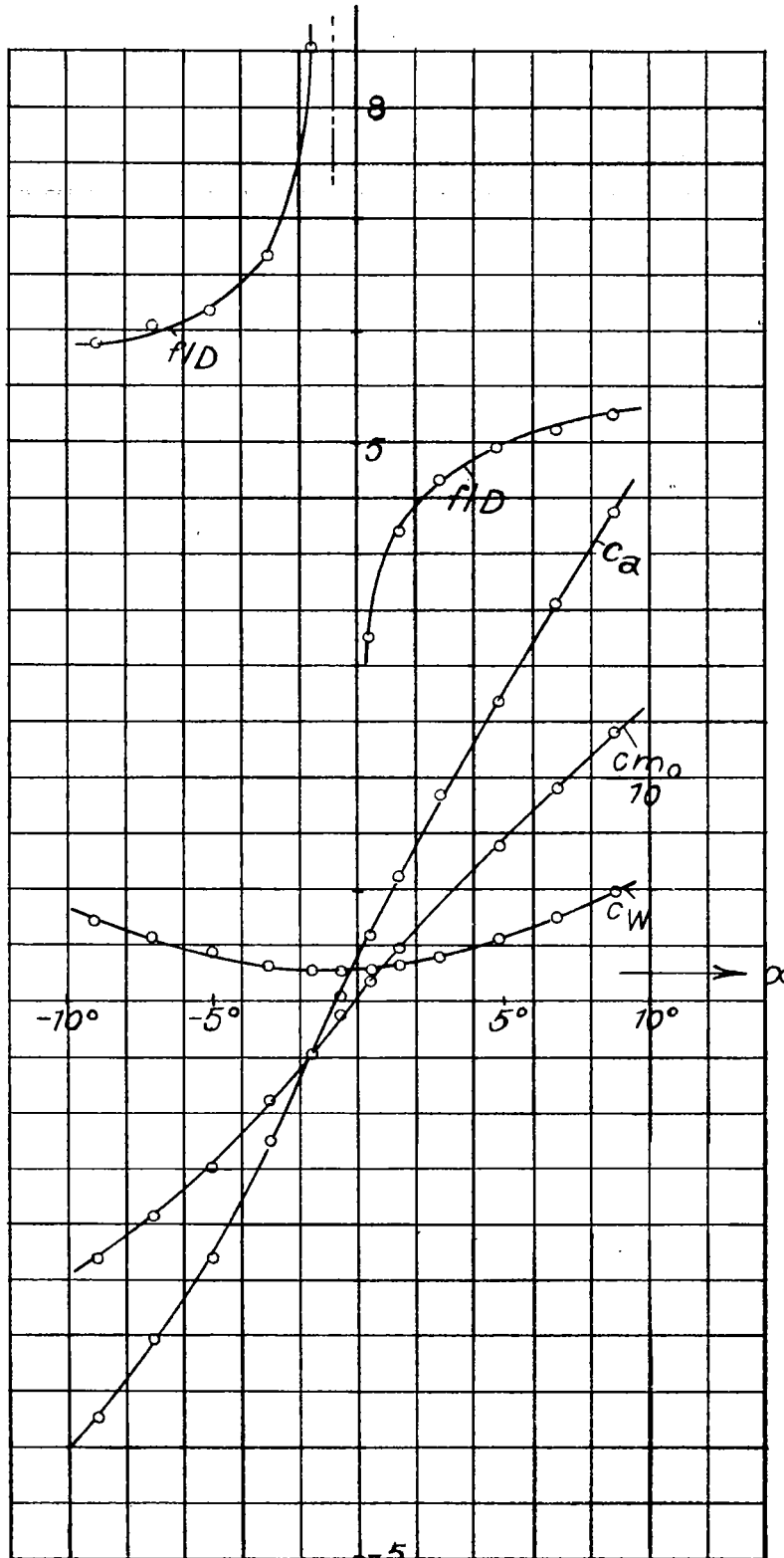Figure 14.- With deflected rudder ZR 2.0 M = 0.7.
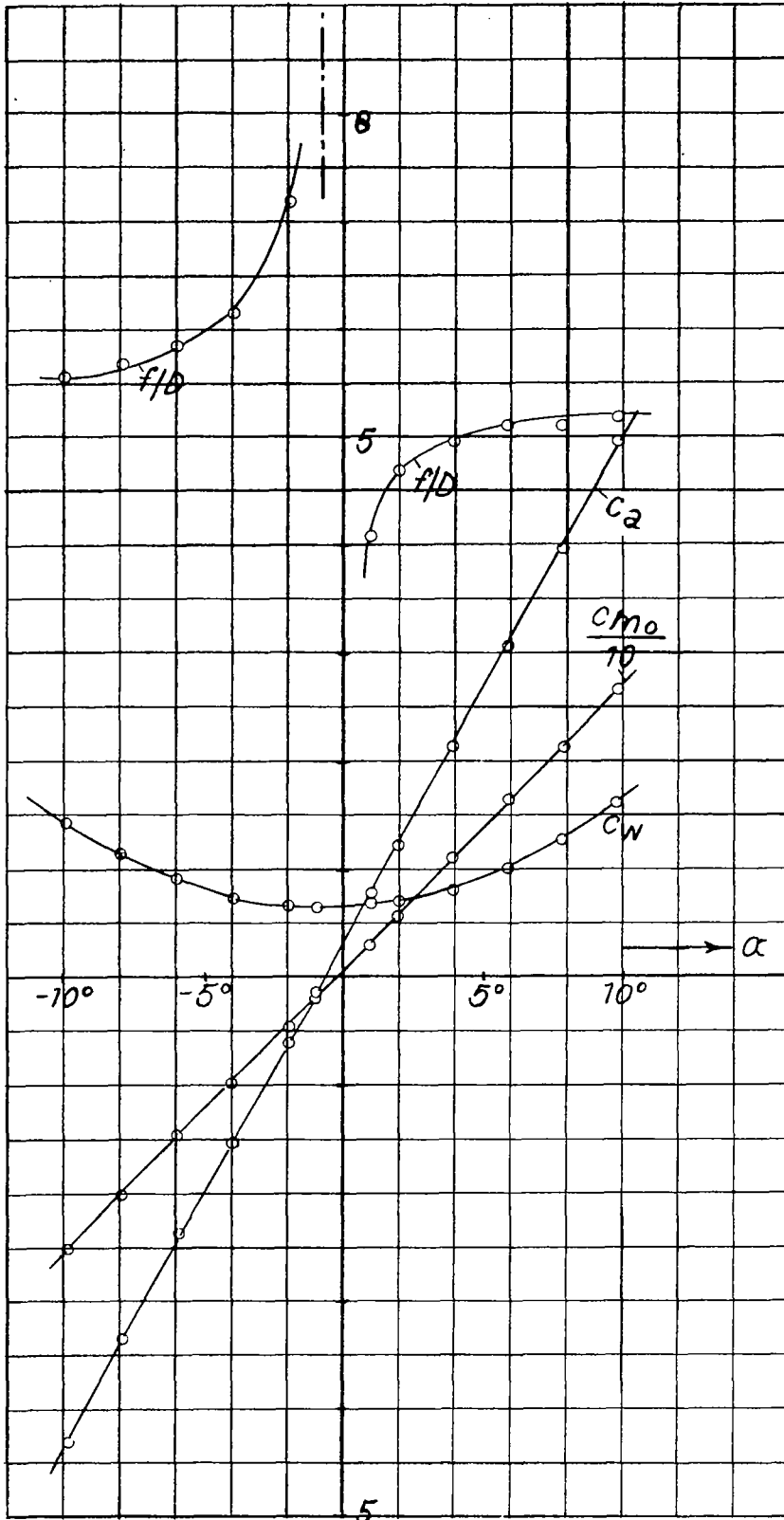
Figure 15.- With deflected rudder ZR 2.0 M = 0.85.

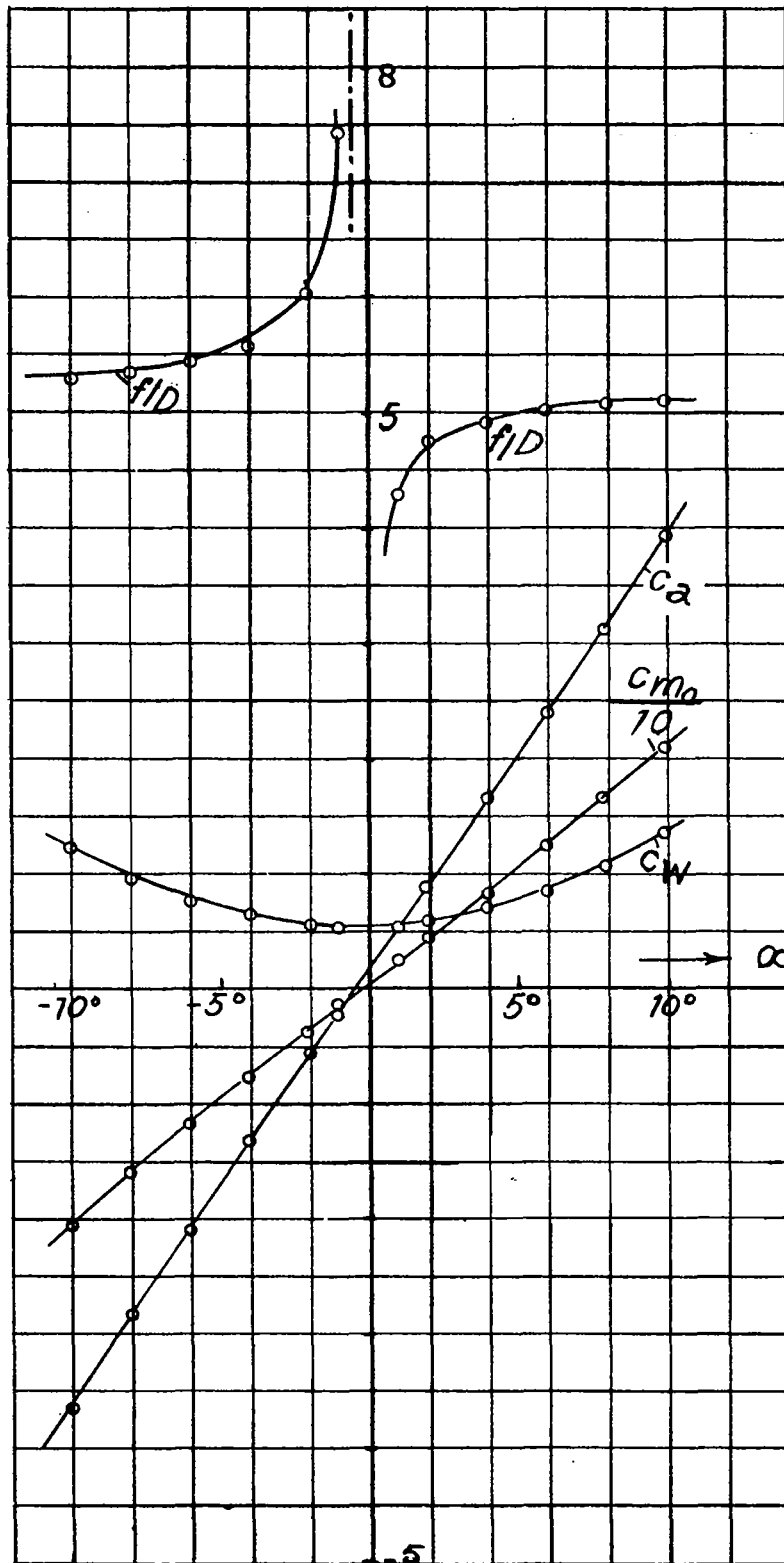Figure 16.- With deflected rudder ZR 2.0 M = 1.45.

Figure 17.- With deflected rudder ZR 2.0 M = 1.99.

NATIONAL ADVISORY COMMITTEE FOR AERONAUTICS

TECHNICAL MEMORANDUM NO. 1159

WIND-TUNNEL MEASUREMENTS ON THE WING OF THE

HENSCHEL MISSILE "ZITTERROCHEN"[1] IN

SUBSONIC AND SUPERSONIC VELOCITIES[#]

By Kehl

Abstract: Supplementing the measured results previously reported, this investigation of three-component measurements on a wing model of the missile "ZR 2.0" was conducted in the subsonic wind tunnel (open-jet 215-millimeter diameter) and in the supersonic wind tunnel (open jet 110 by 130 millimeters) at the request of the Henschel Aircraft Works, Berlin.

Outline: I. Relations and Definitions

II. Description of Model and Measured Results

I. RELATIONS AND DEFINITIONS

A   Lift, component of the air force perpendicular
           to the direction of flow, kilograms

W   drag, component of the air forces in the
           direction of flow, kilograms

[#]"Windkanalmessungen am Flügel des Henschelgerätes 'Zitterrochen' bei Unter- und Überschallgeschwindigkeiten." Zentrale für wissenschaftliches Berichtswesen der Luftfahrtforschung des Generalluftzeugmeisters (ZWB) - Berlin-Adlershof, Untersuchungen und Mitteilungen Nr. 3161. Oct. 24, 1944.

[1]Literally "trembling ray."

M_0 moment, referred to the center of the wing leading edge (tail loaded moment positive), meter-kilograms

F wing area, meters^2

b wing span, meters

l wing chord, meters

l_m mean wing chord, meters $\left(\dfrac{b}{\Lambda}\right)$

ρ air density (kg sec^2 m^{-4})

v stream velocity (m sec^{-1})

a sonic velocity (m sec^{-1})

α angle of attack, degrees

Λ wing aspect ratio $\left(\dfrac{b^2}{F}\right)$

M Mach number $\left(\dfrac{v}{a}\right)$

c_a lift coefficient $\left(\dfrac{A}{\dfrac{\rho}{2}\,v^2 F}\right)$

c_w drag coefficient $\left(\dfrac{W}{\dfrac{\rho}{2}\,v^2 F}\right)$

c_{m_0} moment coefficient $\left(\dfrac{M_0}{\dfrac{\rho}{2}\,v^2 F l_m}\right)$

II. DESCRIPTION OF MODEL AND MEASURED RESULTS

In figure 1 the wing under investigation with $\Lambda = 2$ is sketched. The contours are the biconvex profile formed by two circular arcs. The thickness ratio amounts to 6.3 percent. The wing was tested in two directions; these directions A and B are illustrated in figure 1.

The measurements in the subsonic wind tunnel (open-jet 215-millimeter diameter) at $M = 0.5$, 0.7, and 0.85

were taken, as were measurements in the supersonic
wind tunnel (open jet 110 by 130 millimeters) at $M = 1.20$,
1.45, and 1.99. Angle of attack ranged from $0°$ to $10°$.
The polars and the moment-coefficient curves are given
in figures 2 to 5.

For case A, a decrease in the drag was observed with
increasing Mach number, just as was formerly noticed on
the whole model (see UM 3122), which is traceable to
laminar separation at the low Mach numbers. The
Reynolds number based upon the mean chord l_m amounts
to 3.2×10^5 at $M = 0.5$ and to 4.1×10^5 at $M = 0.85$.
In contrast, the case B shows no Reynolds number or
Mach number effect on $c_{w_{min}}$ over the same velocity range.
In both cases, the lift coefficient increases with
Mach number approximately as required by the Prandtl equation.

As was expected, at supersonic velocities the drag
coefficient decreased with increasing Mach number at the
low values of lift coefficient. Likewise, the lift
coefficient decreased with increasing Mach number for a
constant angle of attack.

The pressure point in supersonic as well as subsonic
flow is independent of Mach number over the range of
velocities investigated. In supersonic flow, however,
the pressure point lies farther to the rear than in
subsonic flow.
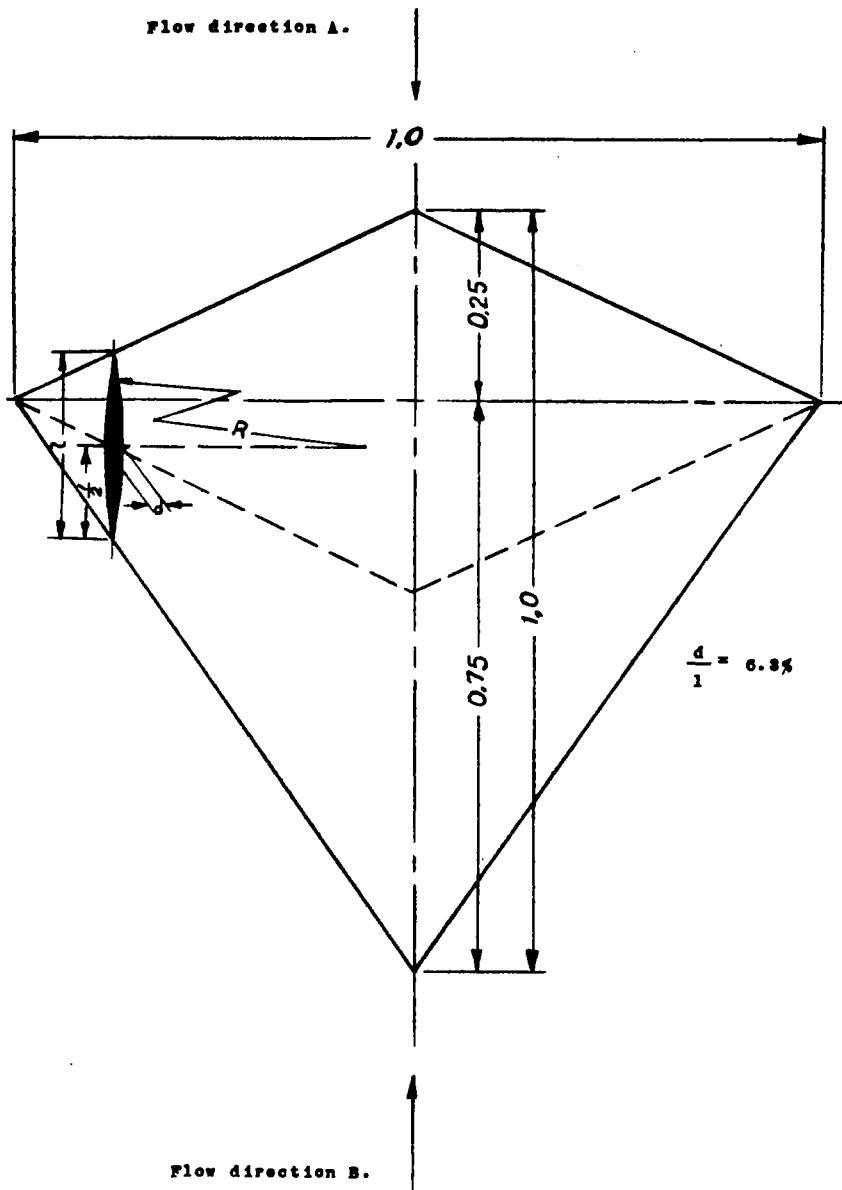
Translated by Chance Vought
Aircraft Corporation

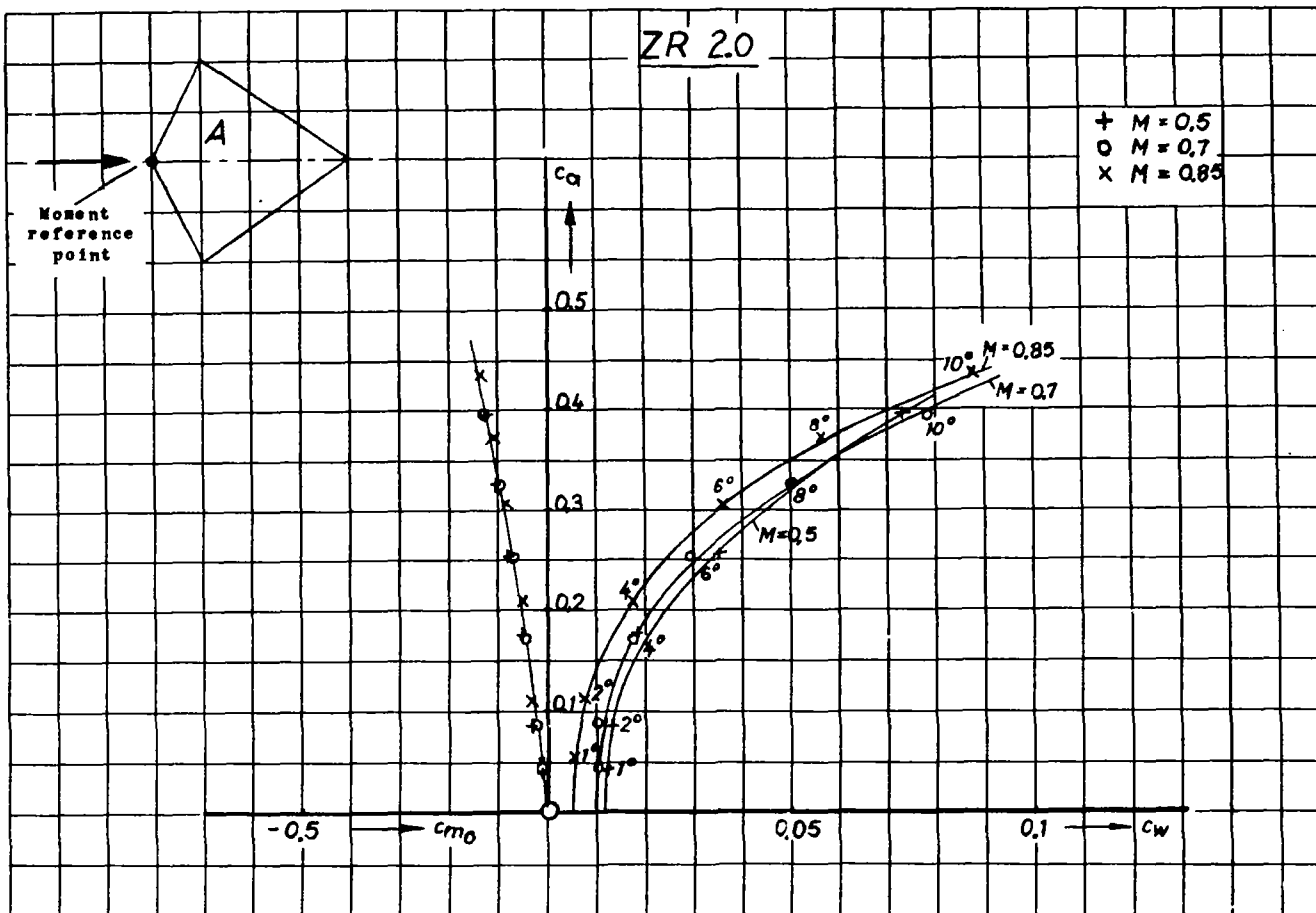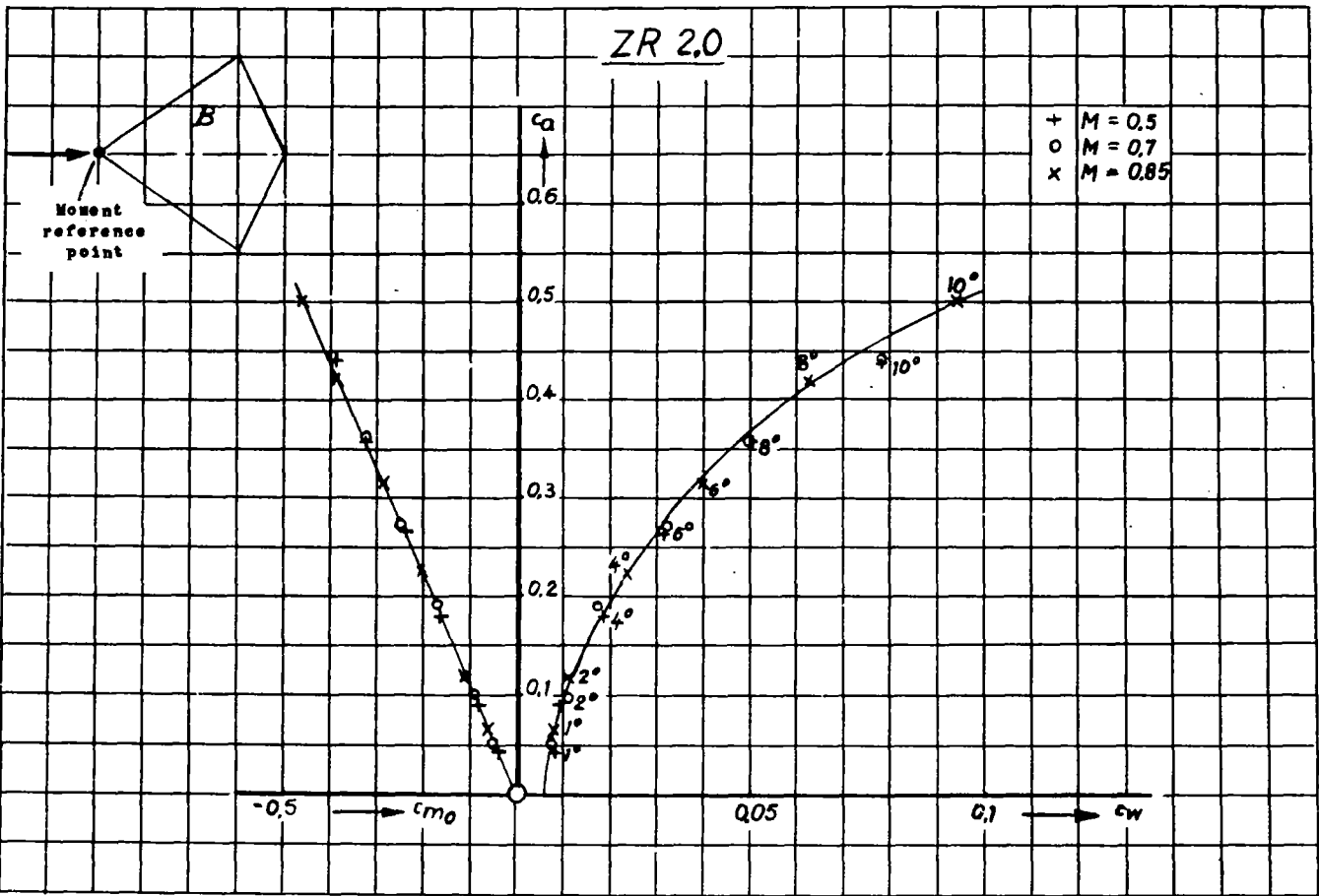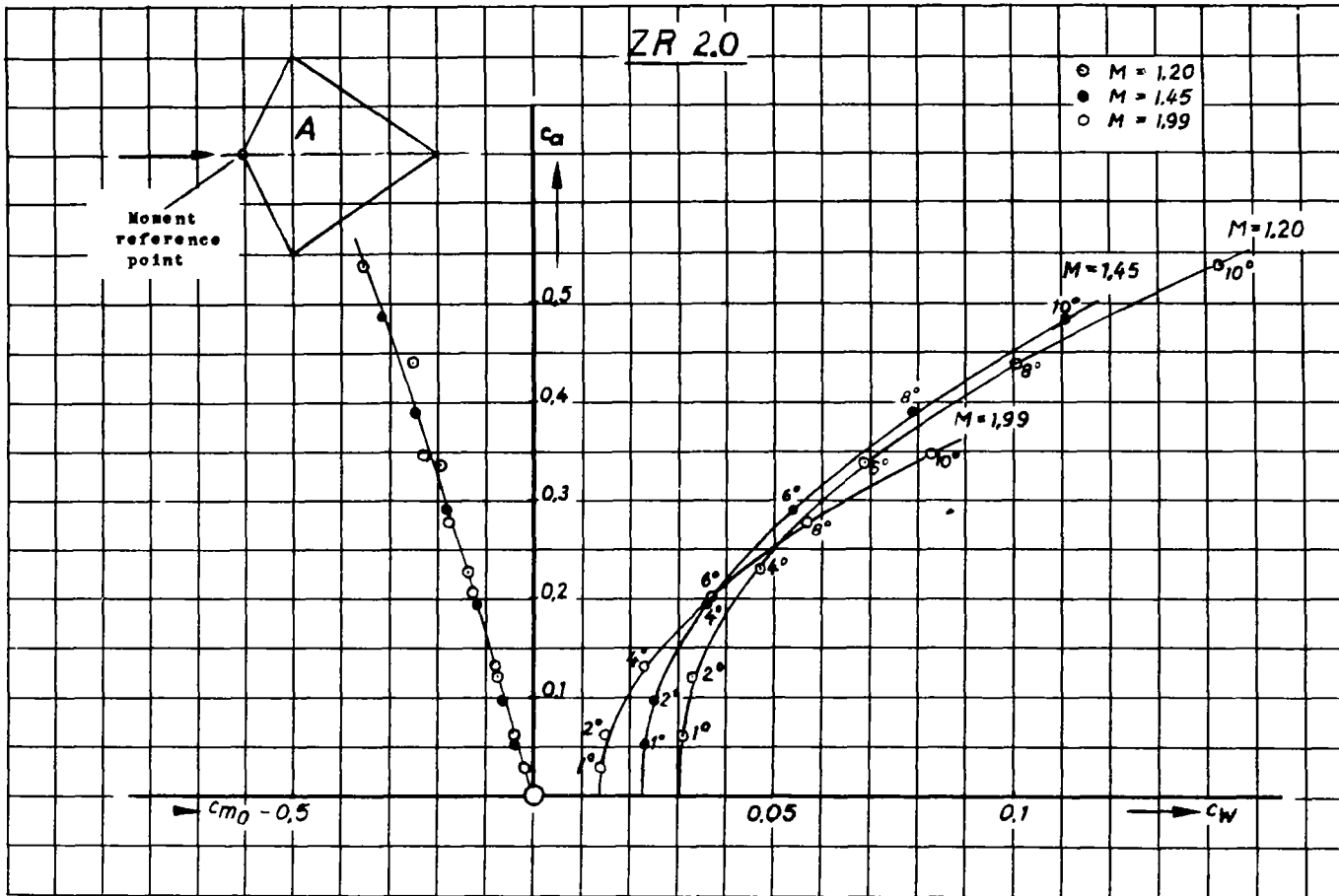Flow direction A.
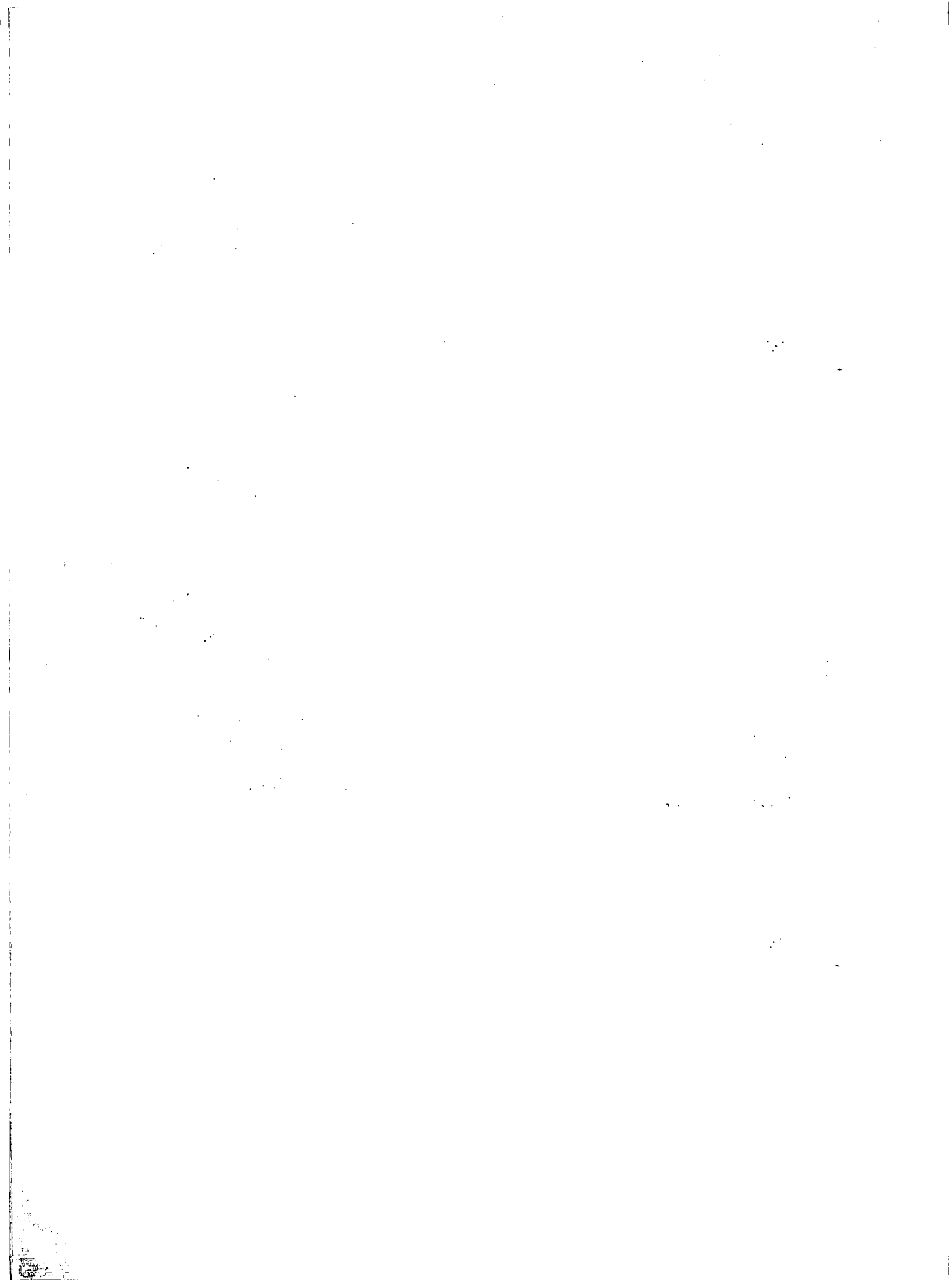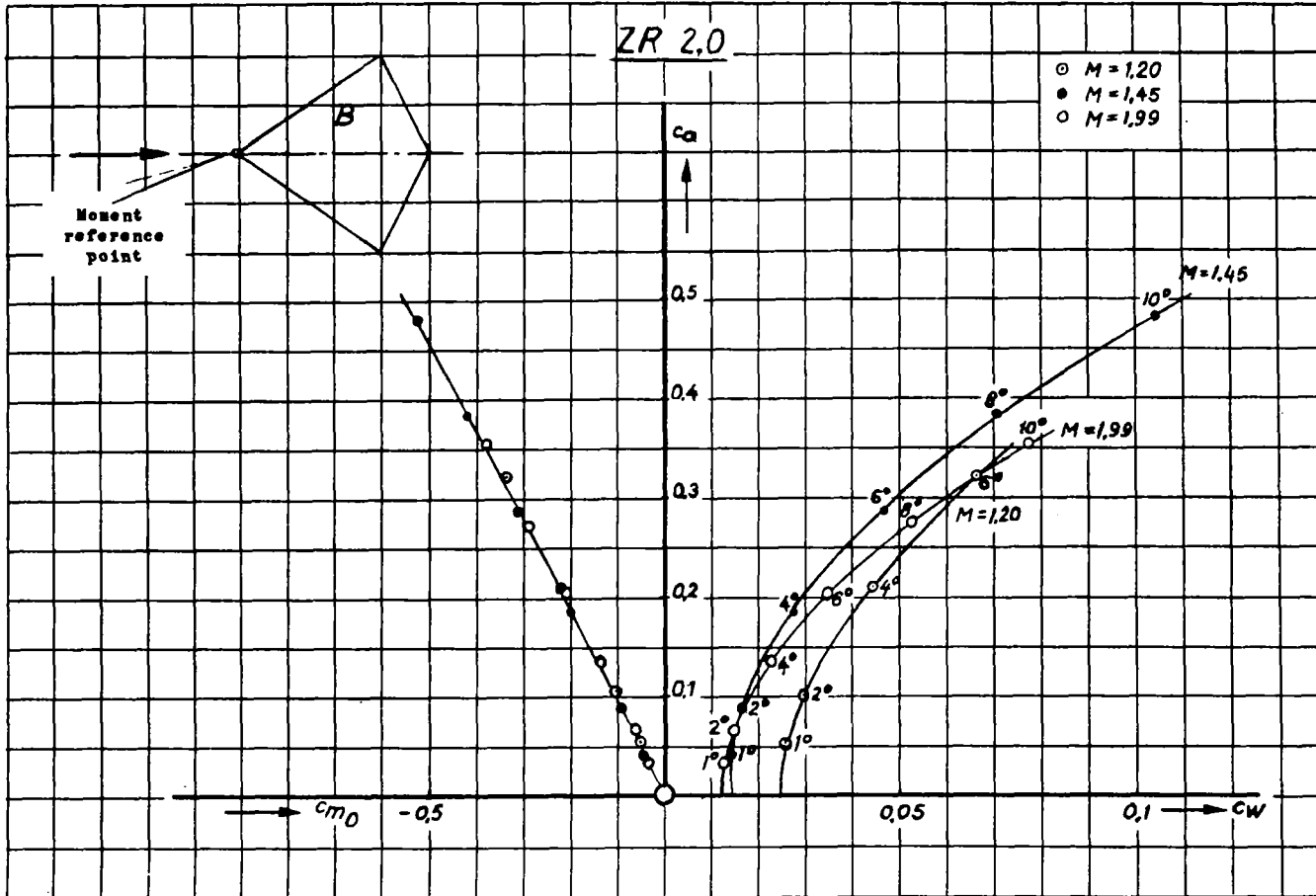

Figure 1.- Wing ZR 2.0; ⋀ = 2.0.

Figure 2.

Figure 3.

Figure 4.

Figure 5.